Investigation of latent heat of melting and thermal conductivity of the low-melting Bi-Sn-Zn eutectic alloy

I. Manasijević[1]* , Lj. Balanović[1], D. Minić[2], M. Gorgievski[1], U. Stamenković[1]

[1] *University of Belgrade, Technical Faculty in Bor, Bor, Serbia*
[2] *University of Priština, Faculty of Technical Sciences, Kosovska Mitrovica, Serbia*

Abstract

Low-melting eutectic alloys represent promising candidates for production of phase change materials (PCMs). PCMs are widely used in the field of thermal energy storage (TES). The most important advantages of the low-melting metallic materials as PCMs are their high volumetric latent heat and high thermal conductivity. However, essential thermophysical properties such as melting point, latent heat of fusion, specific heat capacity, thermal conductivity, and surface tension for many low-melting eutectic alloys are still unknown.

In this study, melting temperature, latent heat of melting and thermal conductivity of the Bi-Sn-Zn eutectic alloy were experimentally investigated. Melting temperature and latent heat of melting were determined by using differential scanning calorimetry (DSC) and compared with the results of thermodynamic calculation according to CALPHAD (calculation of phase diagram) method. Thermal diffusivity of the investigated eutectic alloy at 25 °C was measured by using the xenon-flash method. Based on the experimentally determined thermal diffusivity and the specific heat capacity obtained by thermodynamic calculation, the thermal conductivity of the investigated eutectic alloy was determined to be $22.88 \pm 1.83 \, \mathrm{W \, m^{-1} \, K^{-1}}$. In addition, the microstructure of the investigated eutectic alloy was examined using scanning electron microscopy (SEM) with energy dispersive X-ray spectrometry (EDS).

K e y   w o r d s: Bi-Sn-Zn system, eutectic alloy, latent heat of melting, thermal conductivity

1. Introduction

The alloys based on low-melting metals Sn, Zn, and Bi have been broadly studied and commercially implemented in lead-free soldering [1]. Sn-9Zn eutectic alloy has melting temperature (198 °C) close to that of Sn-Pb eutectic alloy (183 °C) and exhibits better mechanical properties than the conventional Sn-Pb solders. The addition of Bi to the Sn-Zn eutectic alloy further improves its soldering properties, such as joining strength, wettability, and lowers the melting temperature [2, 3].

Phase diagram of the Bi-Sn-Zn ternary system has been thermodynamically assessed by Malakhov et al. [4] and Moelans et al. [5]. The latest thermodynamic optimization of the Bi-Sn-Zn ternary system has been performed by Vizdal et al. [6]. In that work, authors incorporated the newest thermodynamic descriptions of the constitutive binary systems and the results of experimental studies by Luef et al. [7] and Braga et al. [8].

Optimized phase diagram by Vizdal et al. [6] reveals appearance of one ternary eutectic reaction in the Bi-Sn-Zn system with the temperature of the eutectic reaction at 131.7 °C and eutectic composition 35.5Bi-60.1Sn-4.4Zn (at.%). The alloy with the exact eutectic composition corresponds to the alloy with the lowest melting temperature in the ternary Bi-Sn-Zn system, and it could be of interest for the development of metallic phase change materials (PCMs). Phase change materials (PCMs) are materials with a high heat of fusion which undergo melting/solidification process at a constant or nearly constant temperature and absorb/release thermal energy from/to the surroundings [9]. PCMs have widespread usage in the field of thermal management and thermal energy stor-

*Corresponding author: e-mail address: ivanamanasijevic80@gmail.com

T a b l e 1. Thermophysical properties of pure metals Bi, Sn, and Zn 15]

Metal	Melting point (°C)	Latent heat of fusion (J g^{-1})	Density (g cm^{-3})	Specific heat capacity (J g^{-1} K^{-1})	Thermal conductivity (W m^{-1} K^{-1})
Bi	271.4	53.976	9.808 at 25 °C	0.122 at 25 °C	8.2 at 25 °C
Sn	231.9	59.6	7.168 at 25 °C	0.205 at 25 °C	62.8 at 0 °C
Zn	420.0	100.9	7.133 at 25 °C	0.382 at 20 °C	113.0 at 25 °C

age [9–11]. Low melting point metals (LMPMs) and eutectic alloys are a relatively new category of PCMs [12–14]. Their key advantages over other types of non--metallic PCMs are high thermal conductivity and high volumetric latent heat [13, 14]. Thermophysical properties such as melting point, latent heat of fusion, specific heat capacity, and thermal conductivity for pure metals can be found in reference literature [15] (Table 1). They are also available for many solder alloys [16]. However, these data are still unknown for many low-melting eutectic alloys with potential for usage in the field of thermal energy storage [12–14]. One of these alloys is ternary Bi-Sn-Zn eutectic alloy, which is the subject of the present study.

Thus, the aim of this work is an experimental and analytical investigation of microstructure, melting temperature, latent heat of fusion and thermal conductivity for the eutectic alloy from the Bi-Sn--Zn ternary system. For this purpose, prepared alloy with eutectic composition was studied using SEM--EDS, DSC, and thermal conductivity measurements by using the xenon-flash method. Experimentally obtained results were compared with the results of thermodynamic calculation according to the CALPHAD (calculation of phase diagrams) approach.

2. Materials and methods

The Bi-Sn-Zn eutectic alloy with nominal composition 35.5 Bi-60.1 Sn-4.4 Zn (at.%) was prepared by induction melting of pure elements (Bi 99.999 %, Sn 99.99 %, Zn 99.99 %, Alfa Aesar) in the graphite crucible under an argon atmosphere. The mass of the prepared sample was about 4 g. The total mass loss after induction melting was less than 0.2 %.

TESCAN VEGA3 scanning electron microscope with energy dispersive spectroscopy (EDS) (Oxford Instruments X-act) was used for investigation of microstructure, and the analysis was carried out using an accelerating voltage of 20 kV. EDS analysis was applied for the determination of overall and phase compositions of the studied eutectic alloy. SEM images of the microstructure were recorded on the polished surface of the studied alloy in the backscattered electron (BSE) mode.

Simultaneous thermal analyzer SDT Q600 (TA Instruments) was used for measurements of melting temperature and latent heat of melting. Pure metal standards (In and Zn) were used for temperature and heat calibrations. Sample mass was about 50 mg, and a heating rate was 5 °C min^{-1}. DSC heating runs were performed in the temperature interval from 25 to 200 °C and repeated five consecutive times to check the consistency of the results. The reference material was empty alumina crucible.

Thermal diffusivity was measured by using Discovery Xenon Flash (DXF-500) device. For this purpose, a sample of the investigated Bi-Sn-Zn eutectic alloy was shaped by hydraulic pressing into a round disk (12.6 mm in diameter and 2 mm thick with plane-parallel ground end faces). After pressing, the sample was annealed at 100 °C under an inert atmosphere for 5 h in order to remove the internal stresses created during pressing. The DXF-500 device is equipped with nichrome heating elements and an air-cooled aluminium shell [17]. The conducted thermal diffusivity measurements were performed at 25 °C in the vacuumed furnace filled with inert gas. The sample temperature measurements were made by a liquid nitrogen-cooled IR detector [17].

3. Results and discussion

3.1. Thermodynamic analysis

Thermodynamic calculations were carried out using CALPHAD method [18, 19] and the optimized thermodynamic parameters for the Bi-Sn-Zn ternary system from Vizdal et al. [6], included in the COST 531 database [20]. Results of calculations, obtained by using Pandat software [21], include liquidus projection of the Bi-Sn-Zn ternary system, diagram of phase fractions of stable phases as a function of temperature, theoretical enthalpy of fusion, and specific heat capacity for the investigated eutectic alloy.

Figure 1 shows the calculated liquidus projection of the Bi-Sn-Zn ternary system. It includes primary crystallization fields of (Zn), (Sn), (Bi) solid solution phases and liquid miscibility gap in the Zn-rich composition range. Only one ternary invariant reaction of eutectic type appears in the Bi-Sn-Zn ternary system. Eutectic composition corresponds to the point E_1 at the presented liquidus projection.

T a b l e 2. Calculated eutectic temperature and composition of the Bi-Sn-Zn eutectic alloy using the optimized thermodynamic parameters from Ref. [6]

T (°C)	Invariant eutectic reaction	Composition in mole fractions		
		$x(\text{Bi})$	$x(\text{Sn})$	$x(\text{Zn})$
131.7	Liquid $\rightarrow$ (Sn) + (Bi) + (Zn)	0.355	0.601	0.044
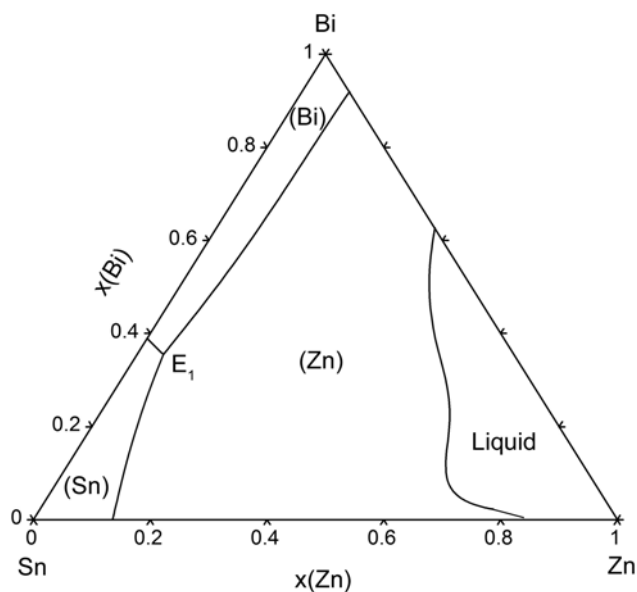
Fig. 1. Calculated liquidus projection of the Bi-Sn-Zn ternary system using thermodynamic parameters from [6].
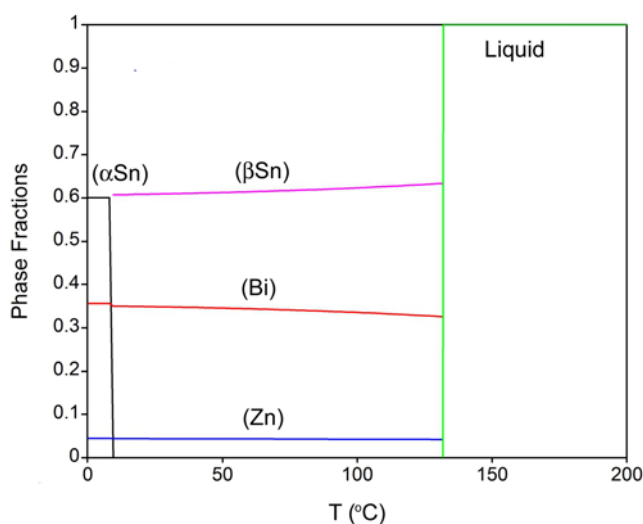
Fig. 2. Calculated phase fractions of stable phases as a function of temperature for the investigated Bi-Sn-Zn eutectic alloy.
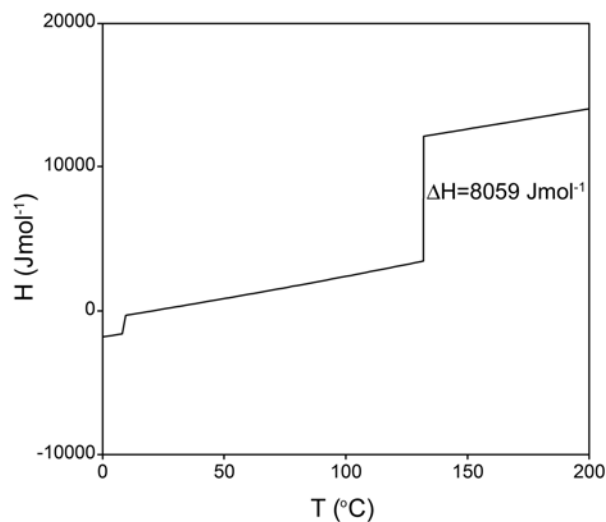

Fig. 3. Calculated temperature dependence of enthalpy for the Bi-Sn-Zn eutectic alloy.

Calculated eutectic temperature and composition of the eutectic alloy are given in Table 2.

Calculated diagram of phase fractions of stable phases as a function of temperature for the eutectic alloy is presented in Fig. 2.

Figure 2 shows the temperature dependence of phase fractions for the Bi-Sn-Zn alloy under equilibrium conditions. Above eutectic temperature (131.7 °C) Bi-Sn-Zn alloy is fully liquid. At the eutectic temperature, liquid phase isothermally decomposes according to the Liquid $\rightarrow$ (Sn) + (Bi) + (Zn) ternary eutectic reaction into the eutectic mixture of (Sn), (Bi), and (Zn) solid solution phases. Immediately below the eutectic temperature, microstructure of the eutectic alloy includes a mixture of (Sn), (Bi), and (Zn) phases. It can be seen that (Sn) phase has the largest phase fraction followed by (Bi) phase and (Zn) phase has a very small phase fraction.

Figure 3 shows the calculated dependence of enthalpy vs. temperature for the investigated Bi-Sn-Zn eutectic alloy. It can be noticed that there is a monotonic increase of enthalpy for the eutectic alloy with temperature increase. This gradual increase is interrupted at the temperatures that correspond to two-phase transformations. At low temperature, there is

T a b l e 3. Comparison of the nominal and experimentally determined overall composition by EDS analysis for the investigated Bi-Sn-Zn eutectic alloy

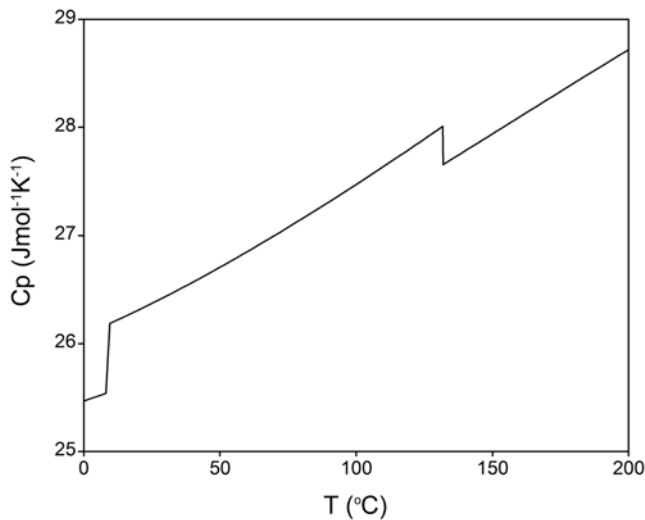| Alloy composition (at.%)					
Bi		Sn		Zn	
Nominal	EDS	Nominal	EDS	Nominal	EDS
35.5	36.5 ± 0.2	60.1	59.5 ± 0.2	4.4	4.0 ± 0.1

Fig. 4. Calculated dependence of specific heat capacity on temperature for the Bi-Sn-Zn eutectic alloy.

the change from (αSn) to (βSn) allotrope. At the eutectic temperature, there is a pronounced rise in enthalpy, caused by melting transformation of the alloy. Enthalpy change during the melting phase transformation represents enthalpy of melting (ΔH_m) or latent heat of melting and is equal to the enthalpy difference between the liquid and solid alloy at the melting temperature. According to the results of the calculation, calculated latent heat of melting for the Bi-Sn-Zn eutectic alloy is 8059.0 J mol^{-1} (54.3 J g^{-1}). This calculated value of latent heat of melting is compared with the results of DSC measurements in the following section of the study.

Calculated specific heat capacity dependence on temperature for the eutectic Bi-Sn-Zn alloy is given in Fig. 4. Similarly to the enthalpy, the specific heat capacity of the investigated eutectic alloy increases with the temperature increase and shows two characteristic steps at phase transformation temperatures.

Since specific heat capacities of the ternary Bi-Sn-Zn alloys have not been experimentally investigated in previous literature, the accuracy of the specific heat capacity calculation was checked by comparing calculated value for the binary Bi-Sn eutectic alloy with

the corresponding known literature value. The calculated value of the specific heat capacity for the Bi-Sn eutectic alloy at 25 °C is 0.169 J g^{-1} K^{-1}, which is in very good agreement with the widely accepted value (0.167 J g^{-1} K^{-1}) for the commercial Bi-Sn eutectic alloy [22]. Thus, it can be concluded that predicted values of specific heat capacity using optimized thermodynamic parameters from [6] own very high accuracy.

The calculated value of specific heat capacity for the investigated Bi-Sn-Zn eutectic alloy at 25 °C is 0.178 J g^{-1} K^{-1}. This value was used for the determination of thermal conductivity in the next part of the study (Section 3.4).

3.2. Microstructure investigation

The microstructure of the prepared Bi-Sn-Zn eutectic alloy was studied using scanning electron microscopy (SEM) combined with energy dispersive X-ray spectroscopy (EDS).

As the first step, the overall composition of the alloy was checked by mapping a large part of the polished surface of the sample (five positions in different regions of the sample were analysed). Nominal composition and experimentally determined average overall composition with standard uncertainties for the investigated Bi-Sn-Zn sample are shown in Table 3 for comparison.

As can be seen from Table 3, there is a reasonable agreement between alloy nominal (target) composition and corresponding composition determined by EDS analysis.

Characteristic SEM micrographs of the investigated Bi-Sn-Zn eutectic alloy are given in Figs. 5a,b. Micrographs of the eutectic alloy reveal a large number of interconnected and irregularly distributed lamellae of the (Bi) phase (bright areas) in the fine-grained matrix based on Sn and Zn (grey areas).

3.3. Measurements of melting temperature and latent heat of melting

Measurements of melting (eutectic) temperature and latent heat of melting for the investigated Bi-Sn-Zn eutectic alloy were done using differential scanning

T a b l e 4. Comparison between results of thermodynamic calculation and DSC results for the investigated Bi-Sn-Zn eutectic alloy

Calculation		Experimental results	
Melting temperature (℃)	Latent heat of melting (J g^{-1})	Melting temperature (℃)	Latent heat of melting (J g^{-1})
131.7	54.3	132.4 ± 0.1	44.1 ± 0.2
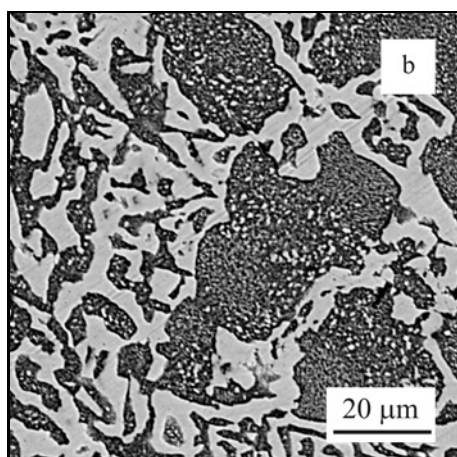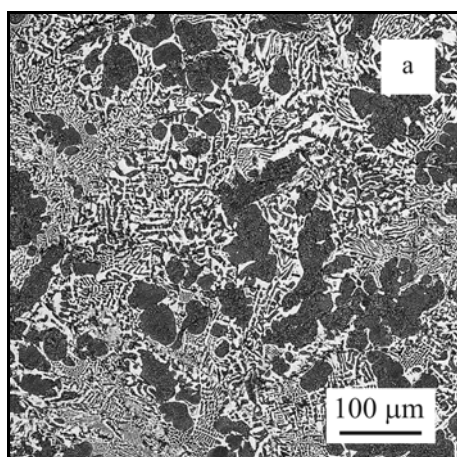
Fig. 5. SEM micrograph of the investigated Bi-Sn-Zn eutectic alloy under different magnifications: (a) 500×; (b) 3000×.

Fig. 6. Example of the DSC heating curve for the investigated Bi-Sn-Zn eutectic alloy.

calorimetry (DSC). The eutectic temperature was determined from the extrapolated temperature of the peak onset [13, 14, 23].

Example of DSC heating curve (obtained in the third heating run) for the investigated Bi-Sn-Zn eutectic alloy is given in Fig. 6.

Mean values of melting temperature and latent heat of melting together with related standard uncertainties obtained from repeated DSC heating runs are presented in Table 4.

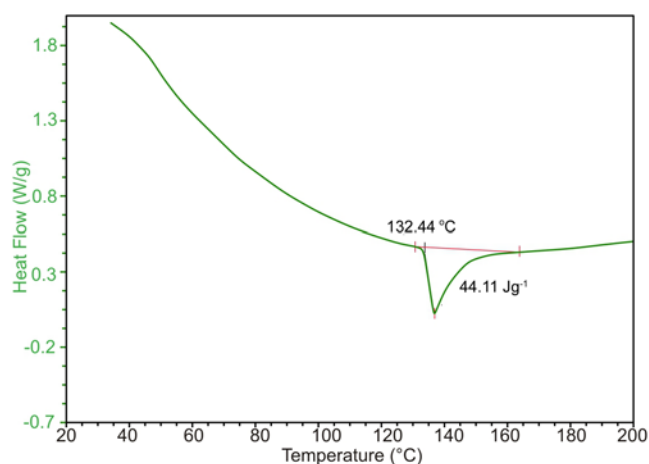Experimentally determined melting temperature and latent heat of melting for the Bi-Sn-Zn eutectic alloy are 132.4 ℃ and 44.1 J g^{-1}, respectively. Melting temperature obtained by DSC measurements (132.4 ℃) is slightly higher than the related calculated value (131.7 ℃). Measured latent heat of melting (44.1 J g^{-1}) is to some extent smaller than related calculated value (54.3 J g^{-1}). Recently, melting temperature and latent heat of melting of the ternary Bi-In-Sn eutectic alloys have been investigated by Manasijević et al. [13]. By using DSC method under the similar experimental conditions, they have determined melting temperature 76.6 ℃ and heat of melting 32.6 J g^{-1} for the 53.8% Bi-27.0% In-19.2% Sn (wt.%) eutectic alloy. For the 32.0% Bi-51.2% In-16.8% Sn (wt.%) alloy, determined melting temperature was 60.8 ℃ and latent heat of melting obtained from DSC heating runs was 25.4 J g^{-1}. It can be noticed that Bi-Sn-Zn eutectic alloy investigated in this work has considerably higher melting temperature and latent heat of melting than ternary Bi-In-Sn eutectic alloys.

Based on the results obtained in this study and previously published results [13, 14] it can be generalized that Bi-based eutectic alloys have melting temperatures that are very usable in the field of low temperature operating metallic PCMs. They are also characterized by relatively low values of latent heat based on the weight compared to the gallium-based eutectic alloys and organic PCMs such as paraffins [11, 12].

T a b l e 5. Specific heat capacity, density, thermal diffusivity and thermal conductivity of the investigated Bi-Sn-Zn eutectic alloy at 25 °C

Alloy (at.%)	Calculated specific heat capacity, C_p (J g^{-1} K^{-1})	Calculated density, ρ (g cm^{-3})	Thermal diffusivity, α (mm^2 s^{-1})	Thermal conductivity, λ (W m^{-1} K^{-1})
Bi-Sn-Zn alloy	0.178	8.282	15.520 ± 0.466	22.880 ± 1.830

However, their vital characteristic is high latent heat based on the volume. This fact can be very important for the practical application of these alloys in the thermal energy storage systems with small working space.

3.4. Determination of thermal conductivity

Thermal conductivity represents one of the most important thermal properties for the selection and application of PCMs. Thermal conductivity determines the efficiency of the heat transfer during the phase change. So, the accurate data on thermal conductivity is an essential precondition for the design and selection of PCMs. In this study thermal conductivity of the Bi-Sn-Zn eutectic alloy at 25 °C has been determined by using the xenon-flash method.

Xenon-flash technique [24] is based on uniform irradiation of a disc-shaped sample over its front face with a very short pulse of energy. The sample's thermal diffusivity α is calculated using the following Eq. (1) [17, 24]:

$$\alpha = \frac{1.37L^2}{\pi^2 t_{1/2}} = 0.1388 \frac{L^2}{t_{1/2}}, \quad (1)$$

where L represents the thickness of the sample and $t_{1/2}$ is the half-rise time, defined as time interval required for the rear surface temperature to reach half of the maximal temperature increase.

The specific heat capacity C_p of a material represents the amount of energy required to raise a unit mass of material by one unit of temperature at constant pressure:

$$C_p = \frac{Q}{m \Delta T}, \quad (2)$$

where C_p is specific heat capacity (J kg^{-1} K^{-1}), m is mass (kg), ΔT is a change in temperature, and Q is the amount of energy (J).

In this study, the specific heat capacity of the investigated Bi-Sn-Zn eutectic alloy was calculated using optimized thermodynamic parameters from [6] (Fig. 4).

Based on the measured value of the thermal diffusivity and the calculated specific heat capacity value, thermal conductivity of the investigated sample was determined using a relationship given by Parker et al. [24]:

$$\lambda = \alpha \rho C_p, \quad (3)$$

where λ is thermal conductivity (W m^{-1} K^{-1}), α is thermal diffusivity (m^2 s^{-1}), ρ is density (kg m^{-3}), and C_p is specific heat capacity (J g^{-1} K^{-1}).

Alloy density at 25 °C is estimated from the density values of pure constitutive metals [15] using relationship:

$$\frac{100}{\rho_{\text{BiSnZn}}} = \frac{\text{wt.\%Bi}}{\rho_{\text{Bi}}} + \frac{\text{wt.\%Sn}}{\rho_{\text{Sn}}} + \frac{\text{wt.\%Zn}}{\rho_{\text{Zn}}}. \quad (4)$$

Calculated density of the investigated Bi-Sn-Zn eutectic alloy at 25 °C is 8.282 g cm^{-3}, which is somewhat lower than reported density for the Bi-Sn eutectic alloy (8.56 g cm^{-3}) [12].

The obtained values of thermal diffusivity, specific heat capacity, and thermal conductivity for the Bi-Sn-Zn eutectic alloy at room temperature (25 °C) are given in Table 5. The uncertainty of the thermal diffusivity measurements is estimated to be ± 3 % and the uncertainties of the specific heat capacities according to the thermodynamic calculation and density determination are estimated to be ± 5 % [25]. The total uncertainty for the thermal conductivity is estimated to be ± 8 %.

The thermal conductivity of Bi-Sn-Zn eutectic alloy at 25 °C is 22.88 ± 1.83 W m^{-1} K^{-1}, which is higher than the thermal conductivity of pure bismuth, but considerably lower than thermal conductivities of pure tin and zinc (Table 1). The obtained value of thermal conductivity for the Bi-Sn-Zn eutectic alloy is only slightly higher than reported thermal conductivity for the Bi-Sn eutectic alloy (19 W m^{-1} K^{-1}) [12] and significantly lower than thermal conductivity of Sn-Zn eutectic alloy (61 W m^{-1} K^{-1}) [12], and Sn-Ag eutectic alloy (84.6 W m^{-1} K^{-1}) [26].

4. Conclusions

Thermal properties including melting temperature, latent heat of melting, thermal diffusivity, specific heat capacity, and thermal conductivity of the Bi-Sn-Zn eutectic alloy were examined in this study. The composition of the investigated eutectic alloy was chosen according to the latest Bi-Sn-Zn phase diagram proposed in the literature. Based on the obtained results from this work following conclusions can be made:

– Thermodynamic calculations were successfully used for the construction of phase fractions vs. tempe-

rature diagram and for the calculation of theoretical latent heat of melting and specific heat capacity for the investigated Bi-Sn-Zn eutectic alloy.

– The microstructure of the investigated eutectic alloy is characterized by the irregularly distributed lamellae of the (Bi) phase and the fine-grained mixture of (Sn) and (Zn) phases.

– Measured melting temperature is $132.4 \pm 0.1\,°C$, which is slightly higher than calculated value $131.7\,°C$. Experimentally determined latent heat of melting $(44.1 \pm 0.2 \text{ J g}^{-1})$ is lower than the thermodynamically calculated enthalpy of melting (54.3 J g^{-1}).

– Based on the measured thermal diffusivity and calculated specific heat capacity values, the thermal conductivity of the investigated alloy at $25\,°C$ was determined to be $22.88 \pm 1.83 \text{ W m}^{-1} \text{ K}^{-1}$, which is quite low in comparison with other non-bismuth eutectic alloys.

The results of an experimental and analytical investigation of the Bi-Sn-Zn eutectic alloy could be useful for deeper insight into the thermal properties of this alloy as candidate metallic PCM.

Acknowledgement

References

[1] Debski, A., Onderka, B., Gasior, W., Gancarz, T.: Arch. Metall. Mater., *62*, 2017, p. 1945. doi:10.1515/amm-2017-0292

[2] El-Daly, A. A., Swilem, Y., Makled, M. H., El--Shaarawy, M. G., Abdraboh, A. M.: J. Alloy Compd., *484*, 2009, p. 134. doi:10.1016/j.jallcom.2009.04.108

[3] Mladenović, S., Manasijević, D., Gorgievski, M., Minić, D., Dimitrijević, S.: Metall. Mater. Eng., *23*, 2017, p. 11. doi:10.30544/259

[4] Malakhov, D. V., Liu, X. J., Ohnuma, I., Ishida, K.: J. Phase Equilib., *21*, 2000, p. 514. doi:10.1007/s11669-000-0019-1

[5] Moelanes, N., Kumar, K. C. H., Wollantes, P.: J. Alloy Compd., *360*, 2003, p. 98. doi:10.1016/S0925-8388(03)00325-6

[6] Vizdal, J., Braga, M. H., Kroupa, A., Richter, K. W., Soares, D., Malheiros, L. F., Ferreira, J.: Calphad, *31*, 2007, p. 438. doi:10.1016/j.calphad.2007.05.002

[7] Luef, C., Paul, A., Vizdal, J., Kroupa, A., Kodentsov, A., Ipser, H.: Monatsh. Chem., *137*, 2006, p. 381. doi:10.1007/s00706-005-0457-x

[8] Braga, M. H., Vizdal, J., Kroupa, A., Ferreira, J., Soares, D., Malheiros, L. F.: Calphad, *31*, 2007, p. 468. doi:10.1016/j.calphad.2007.04.004

[9] Yang, X. H., Tan, S. C., Liu, J.: Int. J. Heat Mass Tran., *100*, 2016, p. 899. doi:10.1016/j.ijheatmasstransfer.2016.04.109

[10] Yang, X. H, Tan, S. C., Ding, Y. J., Wang, L., Liu, J., Zhou, Y. X.: Int. Commun. Heat Mass., *87*, 2017, p. 118. doi:10.1016/j.icheatmasstransfer.2017.07.001

[11] Fleischer, A. S.: Thermal Energy Storage Using Phase Change Materials: Fundamentals and Applications. Cham, Springer 2015. doi:10.1007/978-3-319-20922-7

[12] Ge, H., Li, H., Mei, S., Liu, J.: Renew. Sust. Energ. Rev., *21*, 2013, p. 331. doi:10.1016/j.rser.2013.01.008

[13] Manasijević, I., Balanović, Lj., Holjevac Grgurić, T., Minić, D., Gorgievski, M.: Mater. Res.-Ibero-Am J., *21*, 2018, e20180501. doi:10.1590/1980-5373-MR-2018-0501

[14] Manasijević, I., Balanović, Lj., Holjevac Grgurić, T., Minić, D., Gorgievski, M.: J. Therm. Anal. Calorim., *136*, 2019, p. 643. doi:10.1007/s10973-018-7679-8

[15] ASM Handbook Volume 2: Properties and Selection: Nonferrous Alloys and Special-Purpose Materials. Materials Park, ASM International 1990.

[16] Wu, Y. K., Lin, K. L., Salam, B.: J. Electron. Mater., *38*, 2009, p. 227. doi:10.1007/s11664-008-0589-y

[17] Manasijević, D., Radović, Ž., Štrbac, N., Balanović, Lj., Stamenković, U., Gorgievski, M., Minić, D., Premović, M., Holjevac Grgurić, T., Tadić, N.: Mater. Test., *60*, 2018, p. 1175. doi:10.3139/120.111268

[18] Saunders, N., Miodownik, A. P.: CALPHAD (A Comprehensive Guide). London, Elsevier 1998.

[19] Lukas, H. L., Fries, S. G., Sundman, B.: Computational Thermodynamics: The Calphad Method. Cambridge, Cambridge University Press 2007.

[20] Kroupa, A., Dinsdale, A. T., Watson, A., Vrestal, J., Vízdal, J., Zemanova, A.: JOM, *59*, 2007, p. 20. doi:10.1007/s11837-007-0084-6

[21] Cao, W., Chen, S. L., Zhang, F., Wu, K., Yang, Y., Chang, Y. A., Schmid-Fetzer, R., Oates, W. A.: Calphad, *33*, 2009, p. 328. doi:10.1016/j.calphad.2008.08.004

[22] Available at https://www.americanelements.com/bismuth-tin-alloy

[23] Boettinger, W. J., Kattner, U. R., Moon, K. W., Perepezko, J. H.: DTA and Heat-flux DSC Measurements of Alloy Melting and Freezing. In: Zhao, J. C. (Ed.): Methods for Phase Diagram Determination. Amsterdam, Elsevier Science 2007. doi:10.1016/B978-008044629-5/50005-7

[24] Parker, W. J., Jenkins, R. J., Butler, C. P., Abbott, G. L.: J. Appl. Phys., *32*, 1961, p. 1679. doi:10.1063/1.1728417

[25] Huang, L., Liu, S., Du, Y., Zhang, C.: Calphad, *62*, 2018, p. 99. doi:10.1016/j.calphad.2018.05.011

[26] Meydaneri, F., Saatci, B., Ozdemir, M.: Kovove Mater., *51*, 2013, p. 173. doi:10.4149/km_2013_3_173